Towards Multi-scale Fault/fracture System Modeling

C. Meng (cmeng@mit.edu) C. Gu B. Hager

ERL, MIT

July 1, 2019

Towards Multiscale Fault (zone) Modeling

- Realistic fault networks consist of intersections and off-fault structures;
- intersecting faults are dealt with “cross-link” constraint method;
- off-fault structures are conceptualized as Eshelby’s inclusions.

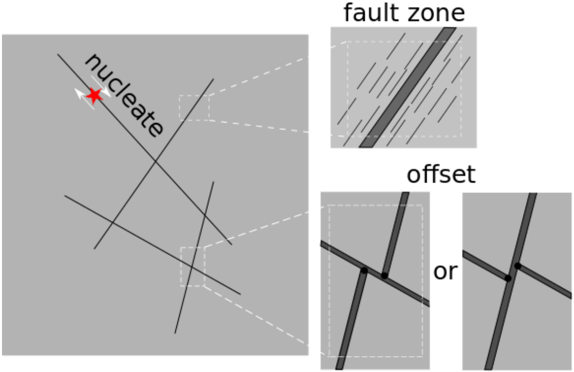

Cross-link constraint method

To model intersecting faults:

- Place cross-link node pairs at the fault intersections;
- fault orientation vectors at the cross-link pairs update according to intersection offset scenarios, no need to change constraint matrix.

[Meng and Hager 2019, in review]

SCEC14/15 modified

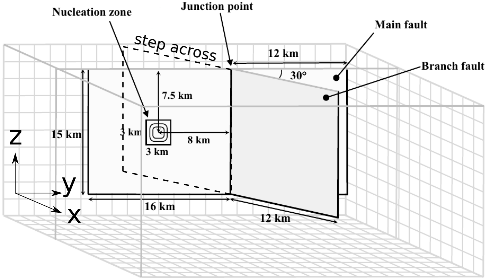

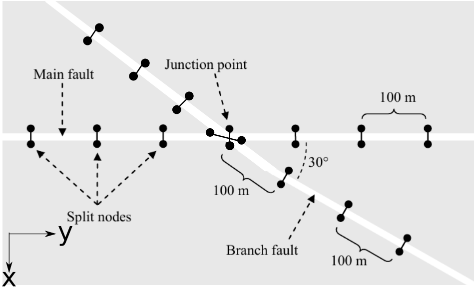

Cross-link illustration

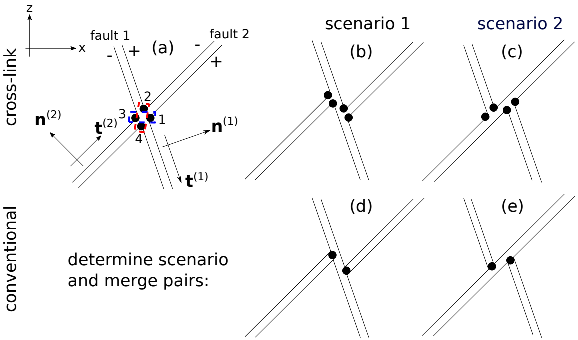

$$\begin{bmatrix} t_x^{(i)} & t_z^{(i)} & 0 & 0 & -t_x^{(i)} & -t_z^{(i)} & 0 & 0 \\ n_x^{(i)} & n_z^{(i)} & 0 & 0 & -n_x^{(i)} & -n_z^{(i)} & 0 & 0 \\ 0 & 0 & t_x^{(i)} & t_z^{(i)} & 0 & 0 & -t_x^{(i)} & -t_z^{(i)} \\ 0 & 0 & n_x^{(i)} & n_z^{(i)} & 0 & 0 & -n_x^{(i)} & -n_z^{(i)} \end{bmatrix} \cdot \begin{bmatrix} u_{1x} \\ u_{1z} \\ u_{2x} \\ u_{2z} \\ u_{3x} \\ u_{3z} \\ u_{4x} \\ u_{4z} \end{bmatrix} = \begin{bmatrix} d^{(i)} \\ l^{(i)} \\ d^{(i)} \\ l^{(i)} \end{bmatrix}, \text{ for } i = 1 \text{ or } 2,$$

Rewrite constraint equations:

$$\begin{bmatrix} t_x^{(i)} & t_z^{(i)} & 0 & 0 \\ n_x^{(i)} & n_z^{(i)} & 0 & 0 \\ 0 & 0 & t_x^{(i)} & t_z^{(i)} \\ 0 & 0 & n_x^{(i)} & n_z^{(i)} \end{bmatrix} \cdot \begin{bmatrix} \mathbf{I} & \mathbf{0} & -\mathbf{I} & \mathbf{0} \\ \mathbf{0} & \mathbf{I} & \mathbf{0} & -\mathbf{I} \end{bmatrix} \cdot \begin{bmatrix} \mathbf{u}_1 \\ \mathbf{u}_2 \\ \mathbf{u}_3 \\ \mathbf{u}_4 \end{bmatrix} = \begin{bmatrix} d^{(i)} \\ l^{(i)} \\ d^{(i)} \\ l^{(i)} \end{bmatrix}, \text{ for } i = 1 \text{ or } 2.$$

The constraint coefficient matrix is fixed, regardless of in which direction the fault shall slip.

$$\begin{bmatrix} \mathbf{I} & \mathbf{0} & -\mathbf{I} & \mathbf{0} \\ \mathbf{0} & \mathbf{I} & \mathbf{0} & -\mathbf{I} \end{bmatrix} \cdot \begin{bmatrix} \mathbf{u}_1 \\ \mathbf{u}_2 \\ \mathbf{u}_3 \\ \mathbf{u}_4 \end{bmatrix} = \begin{bmatrix} t_x^{(i)} & n_x^{(i)} & 0 & 0 \\ t_z^{(i)} & n_z^{(i)} & 0 & 0 \\ 0 & 0 & t_x^{(i)} & n_x^{(i)} \\ 0 & 0 & t_z^{(i)} & n_z^{(i)} \end{bmatrix} \cdot \begin{bmatrix} d^{(i)} \\ l^{(i)} \\ d^{(i)} \\ l^{(i)} \end{bmatrix}, \text{ for } i = 1 \text{ or } 2.$$

The code compares the slip tendency in two directions to determine the RHS.

Example results, modified SCEC 14

When the intersection is offset by fault 1:

- Slip on fault 2 is discontinuous at the intersection;
- two dark lines appear on the last plot.

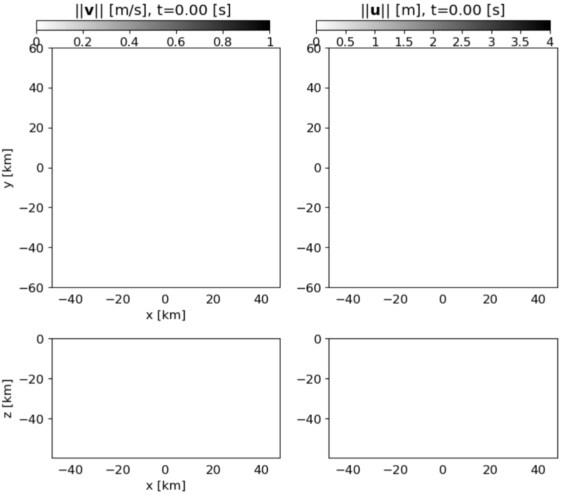

Modified SCEC 15

When the intersecion is offset by fault 2:

- Slip on fault 1 is terminated at the intersection;
- only one dark line appears on the last plot.

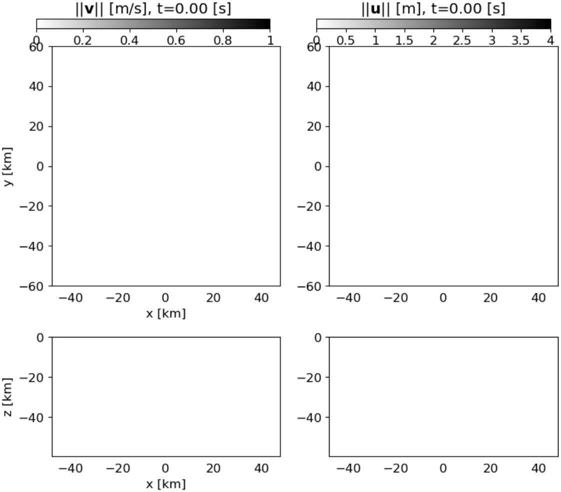

(Equivalent) Eshelby's inclusion problems

- Displacement and stress around a inclusion subject to unconstrained inelastic transformation are given by Eshelby's solution;
- elastic perturbations around an ellipsoidal inhomogeneity excited by uniform loading can be resolved as an equivalent inclusion problem.

(a)

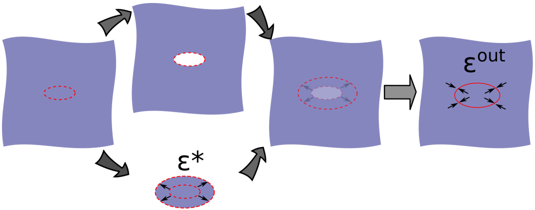

(b)

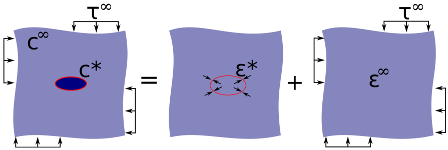

Interactive inhomogeneities

- For single inclusion,
$u_i(\mathbf{x}) = \frac{1}{8\pi(1-\nu)} \left(\psi_{,jli}\epsilon^*_{jl} - 2\nu\epsilon^*_{mm}\phi_{,i} - 4(1-\nu)\epsilon^*_{il}\phi_{,l} \right),$
$\sigma_{ij}(\mathbf{x}) = \begin{cases} C_{ijkl}(S_{klmn}\epsilon^*_{mn} - \epsilon^*_{kl}), & \text{interior,} \\ C_{ijkl}D_{klmn}(\mathbf{x})\epsilon^*_{mn}, & \text{exterior.} \end{cases}$
where **S** and **D** are interior and exterior Eshelby's tensors respectively; and $\boldsymbol{\epsilon}^*$ is effective eigenstrain, where $(\mathbf{C} - \Delta\mathbf{C}\mathbf{S})\boldsymbol{\epsilon}^* = \Delta\mathbf{C}\boldsymbol{\epsilon}^\infty$.
- For *n* inclusions, Meng [2019b, to be submitted] approximates the eigenstrain $\boldsymbol{\epsilon}^*$ of *i*-th inclusion as
$(\mathbf{C} - \Delta\mathbf{C}^i\mathbf{S}^i)\boldsymbol{\epsilon}^{*i} \approx \Delta\mathbf{C}^i \left(\boldsymbol{\epsilon}^\infty + \sum_{j\neq i}^{n} \mathbf{D}^{ij}\boldsymbol{\epsilon}^{*j} \right),$
which is solved directly after rearranging the unknowns.

Eshelby’s solution in truncated space by Esh3D

Cmparison between Esh3D and purely numerical method for three body problem:

- Esh3D only needs to make grid for host matrix, and considers inclusions analytically.
- Purely numerical model has both inclusions and hots matrix discretized.

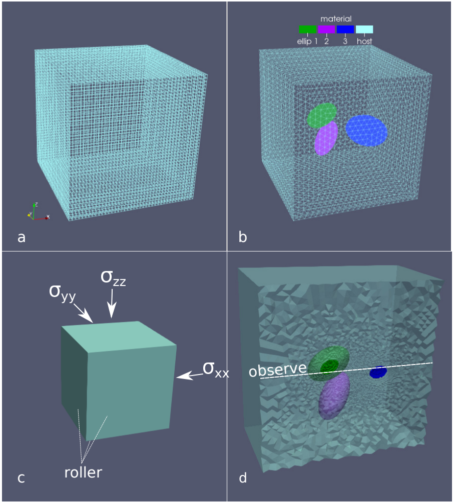

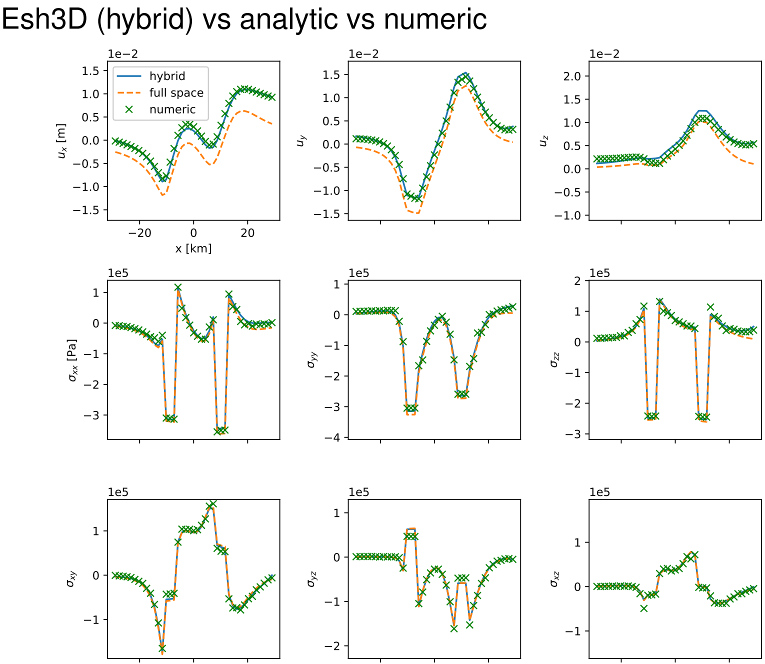

Esh3D (hybrid) vs analytic vs numeric
hybrid
full space
numeric
u_x [m]
u_y
u_z
x [km]
σ_{xx} [Pa]
σ_{yy}
σ_{zz}
σ_{xy}
σ_{yz}
σ_{xz}
1e−2
1e5

The Esh3D code,

- for truncated domain, numerically impose traction (Neumann) and displacement (Dirichlet) boundary conditions [Meng, 2019a];
- for whole space, does not require numerical grid;
- is considerably inexpensive compared to the purely numerical model.

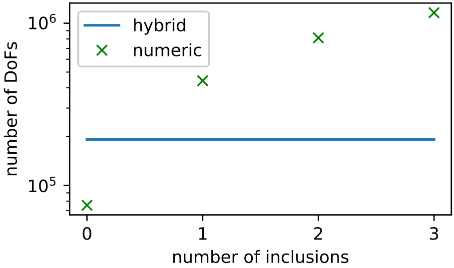

Conceptual fault zone inclusions

- Define a fault zone;
- place ellipsoidal inclusions, with different elastic moduli, in the fault zone;
- the shape, orientation and properties of the inclusions conceptualize off-fault heterogeneous structures.

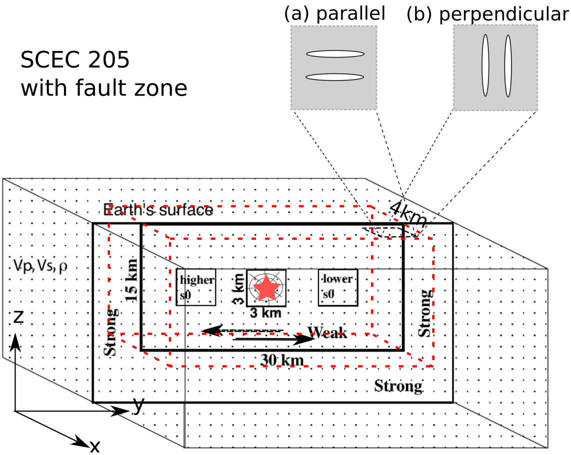

Eshelby's strain in FE weak forms

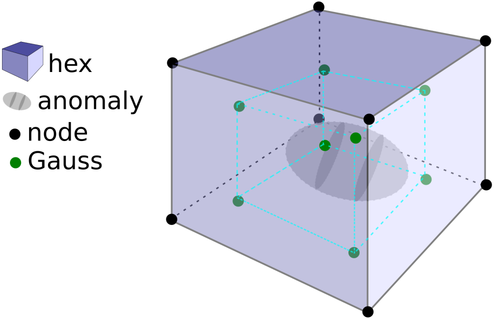

- $[\mathbf{K}] = \sum_j^{n_{\text{Gauss}}} \left[\mathbf{B}^{(j)T} \mathbf{C} \mathbf{D}^{*(j)} \underbrace{\mathbf{B}^{(j)} (\det \mathbf{J} w)^{(j)}}_{\text{total disp} \to \text{strain}} \right]$.
- $\mathbf{D}^{*(\cdot)}$ consists of exterior Eshelby's tensors [Meng et al 2019, to be submitted].

Modified SCEC 205 problem result

Off-fault fracture effects are sensitive to rupture modes:

- Fault-parallel fractures appear to promote mode-III rupture;
- fault-perpendicular fractures appear to retard mode-II rupture.

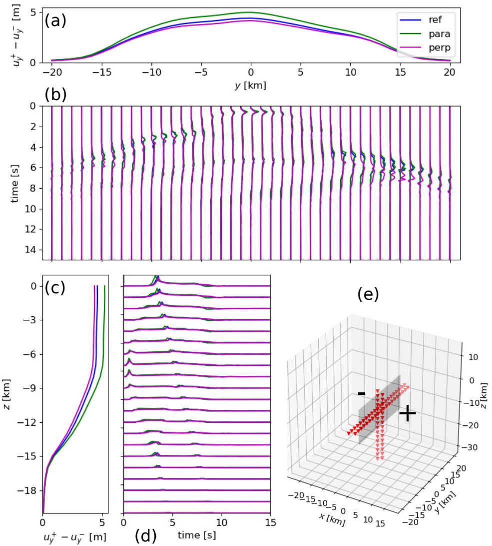

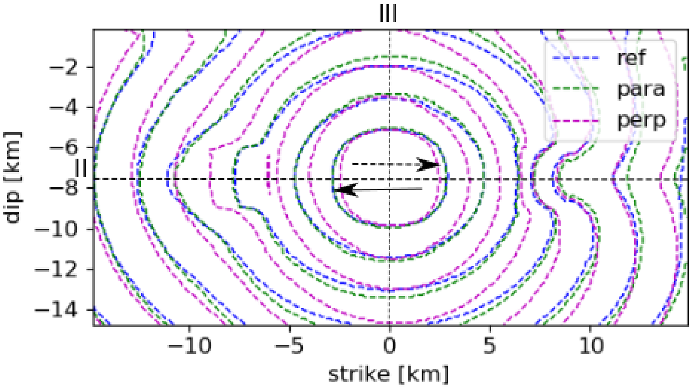

- Horizontally (mode-II), “para” and “ref” stay closely, while “perp” falls behind;
- vertically (mode-III), “ref” and “perp” stay closely, while “para” leads;
- localized mode-III rupture makes “para” advance quicker.

Frequency domain

- first two rows are sampled on the horizontal (mode-II) line;
- third row is sampled on the vertical (mode-III) line.

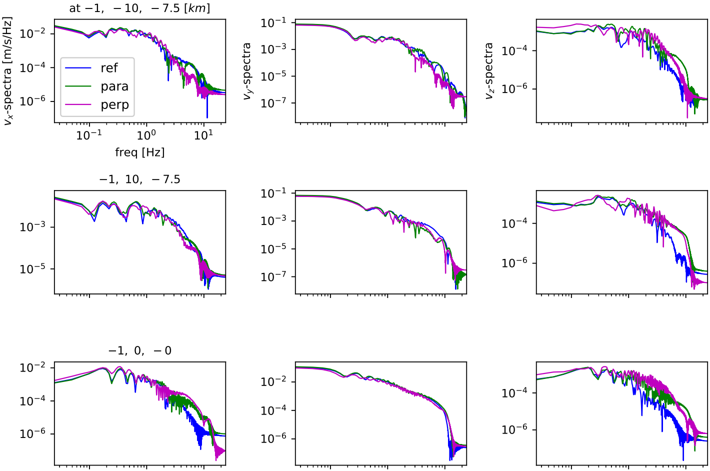

Conclusion

We developed a novel method to efficiently model complex fault (zone) across aseismic and seismic cycles, where

- Intersecting faults are dealt with cross-link constraint method;
- off-fault inhomogeneity is dealt with Eshely's inclusion method.

Static Eshelby's inclusion source can be coupled with Okada's fault source (Esh3D) for joint geodetic data inversion.
Source code:

- `https://github.com/Chunfang/Esh3D`
- `https://github.com/Chunfang/defmod-swpc`